LANGMUIR

Article

pubs.acs.org/Langmuir

Influence of an Additive-Free Particle Spreading Method on Interactions between Charged Colloidal Particles at an Oil/Water Interface

Peng Gao,[†] Zonglin Yi,[‡,§] Xiaochen Xing,[†] To Ngai,[*,‡,§] and Fan Jin[*,†]

[†]Hefei National Laboratory for Physical Sciences at the Microscale, Department of Chemical Physics, Department of Polymer Science and Engineering, CAS Key Laboratory of Soft Matter Chemistry, University of Science and Technology of China, Hefei 230026, PR China

[‡]Department of Chemistry, The Chinese University of Hong Kong, Shatin, N. T. Hong Kong

[§]Shenzhen Municipal Key Laboratory of Chemical Synthesis of Medicinal Organic Molecules, Shenzhen Research Institute, The Chinese University of Hong Kong, Shenzhen 518057, China

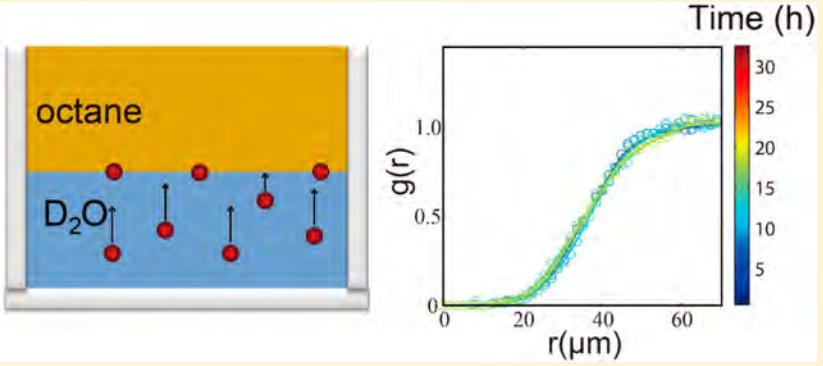

ABSTRACT: The assembly and manipulation of charged colloidal particles at oil/water interfaces represent active areas of fundamental and applied research. Previously, we have shown that colloidal particles can spontaneously generate unstable residual charges at the particle/oil interface when spreading solvent is used to disperse them at an oil/water interface. These residual charges in turn affect the long-ranged electrostatic repulsive forces and packing of particles at the interface. To further uncover the influence arising from the spreading solvents on interfacial particle interactions, in the present study we utilize pure buoyancy to drive the particles onto an oil/water interface and compare the differences between such a spontaneously adsorbed particle monolayer to the spread monolayer based on solvent spreading techniques. Our results show that the solvent-free method could also lead particles to spread well at the interface, but it does not result in violent sliding of particles along the interface. More importantly, this additive-free spreading method can avoid the formation of unstable residual charges at the particle/oil interface. These findings agree well with our previous hypothesis; namely, those unstable residual charges are triboelectric charges that arise from the violently rubbing of particles on oil at the interface. Therefore, if the spreading solvents could be avoided, then we would be able to get rid of the formation of residual charges at interfaces. This finding will provide insight for precisely controlling the interactions among colloidal particles trapped at fluid/fluid interfaces.

1. INTRODUCTION

Micrometer-sized particles trapped at oil/water or air/water interfaces can be easily visualized and continuously tracked via a conventional optical microscope equipped with a video camera. These experimental conveniences offer researchers a quasi-two-dimensional system to directly investigate many fundamental problems in condensed matter physics, such as low-dimensional phase transitions, jamming transitions,[1] crystal melting,[2] and self-assembly[3,4] in which the particles can be viewed as large atoms and their trajectories can be used to elucidate the interactions, thermodynamics, and dynamics in those distinctive phases. Aside from a broad range of applications in fundamental research, understanding and precisely controlling the interfacial interactions among colloidal particles trapped at fluid/fluid interfaces are crucial for Pickering emulsion-related applications, which range from oil recovery[5] to the food industry[6] to fabricating functional porous materials.[7−9]

Therefore, interfacial interactions among colloidal particles trapped at fluid/fluid interfaces, particularly at oil/water interfaces, have been both theoretically and experimentally studied. For example, as early as 1980, Pieranski[10] et al. have shown that, at an air/water interface, interfacial particles can form a two-dimensional colloidal crystal with a lattice constant that is much larger than the particle size, indicating that a long-

Received: April 8, 2016
Revised: April 24, 2016
Published: April 25, 2016

DOI: 10.1021/acs.langmuir.6b01362
Langmuir 2016, 32, 4909−4916

ranged repulsive force exists among those particles at the interface. They suggested that the long-ranged repulsive force arises from long-ranged dipole−dipole interactions at the interface where the asymmetrical dissociation of ion pairs located at particle surfaces results in the formation of dipoles normal to the interface. Thus, the dipole−dipole interaction is highly sensitive to the Debye screening length that is determined by the ionic strength in the aqueous phase. More recently, Petkov et al.[11,12] showed that at an air/water interface the scaling relationship of the surface pressure (Π) and the separation distance (r) between two charged particles at long range is $\Pi \approx r^{-3}$. Also, the scaling relationship of the surface pressure and the average aggregation numbers of particles (n_a) can be represented as $\Pi \approx n_a^{1/2}$. In contrast to the particles trapped at an air/water interface, however, the experimentally measured magnitude of the repulsive force at an oil/water interface has been found to be significantly higher than the theoretical prediction. To understand this discrepancy, Averyard[13,14] et al. measured the long-ranged interactions using optical laser tweezers and suggested that residual charges should exist at the hemisphere of those interfacial particles immersed in the subphase of oil and that add to the electrostatic repulsion. Later, Masschchaele[15] et al. measured the charged colloidal particles trapped at a decane/water interface and proposed that the finite ion size in the compact ion layer or the Stern layer adds to electrostatic interactions. In a recent theoretical study, Uppapalli[16] et al. successfully showed the scaling relationship of the force and the separation distance (r) between two charged particles at both short range (exponential dependence) and long range ($\sim r^{-4}$). More importantly, if we consider that there is a small residual electric charge at the particle/oil interface, the proposed model can quantitatively predict the repulsive force over a large range of the separation distance between two particles.

Indeed, recent experiments also indicated that particles have residual charges in the nonpolar medium,[17] although their origin is elusive. We have recently shown that the quantity of residual charges appearing in oil subphase is highly correlated to the spreading process and that those resultant charges actually are unstable.[18] Those unstable charges will gradually disappear as time evolves, which in turn affects the stability of those particles at interfaces. We proposed that the unstable residual charges are triboelectric charges that arise from the violent rubbing of particles with oil when the particles contact the interface; this is because an instantaneous gradient of surface tension induced by spreading solvents can drive those particles to slide along the interface violently.[19]

It is worth noting that the emergence of those unstable residual charges at particle/oil interfaces leads to a system possessing time-dependent evolution features. This phenomenon may likely limit their fundamental studies, particularly when the required systems need to stay in a thermodynamic equilibrium state. It was explicitly shown in our previous study that the emergence of those unstable residual charges is a side effect arising from the use of spreading solvents. To further reveal the influence led by the spreading solvents upon interaction between charged colloidal particles at an oil/water interface, here we first utilize the buoyancy of microsized particles to drive the particles floating to an oil/D_2O interface. In this way, the use of a spreading solvent can be completely avoided. We then compared the difference between such a spontaneously adsorbed particle monolayer to the spread monolayer obtained from common solvent spreading methods. We found that the additive-free spreading would not lead particles to slide along the interface and thus did not result in time-dependent evolution features among those interfacial particles. Finally, we conclusively demonstrated that the additive-free spreading method is capable of getting rid of the formation of those unstable residual charges at the interface.

2. EXPERIMENTAL SECTION

2.1. Materials. Positively charged 3.5 μm amidine polystyrene (PS) microspheres (Molecular Probes, A37328) were washed three times by spinning down (5000 rpm, 5 min) with a centrifuge and resuspending them in high-purity water (Millipore, 18.2 MΩ·cm). After that, they were suspended in D_2O (Sigma-Aldrich, >99.99%) prior to use. D_2O or octane (Sigma-Aldrich, > 99.999%) was sonicated (30 min) for degassing and further filtered with a syringe filter (Millipore PTFE 0.22 μm).

2.2. Preparation of Horizontal or Vertical Oil/Water Interfaces. The device used to prepare the horizontal or vertical oil/water interfaces is identical to that used in our previous work.[18] Briefly, the device was assembled with a coverslip (thickness 0.17 mm), a PET spacer (thickness 0.1 mm, a hole with 5 mm diameter in the center), and a glass dish (a hole with 1 cm diameter in the center), as shown in Figure 1a. After assembly, 2 μL of D_2O was gently pipetted to fill the hole at the PET spacer. Next, 2 mL of octane was gently pipetted to fill the glass dish. As a result, a horizontal oil/water interface with a thin aqueous phase (0.1 mm) can be well formed in the device. To avoid perturbations from the environment, the device was finely sealed. The device used to prepare the vertical oil/water interfaces contains two coverslips and a PTFE spacer, as shown in Figure 1b. Both coverslips were first treated with 5% HF solution for 20 s, washed with ultrapure water, and then treated with plasma cleaner for 5 min. The resultant surface of treated coverslips is superhydrophilic with a water contact angle approaching 0°. Next, half of the coverslips were treated with a silane coupling agent in toluene. As a result, one side of the coverslip is hydrophilic, and the other side is hydrophobic, where a vertical oil/water interface can be well formed at the boundary. All devices used in this study were assembled by a with silicone glue (Dow Corning 737).

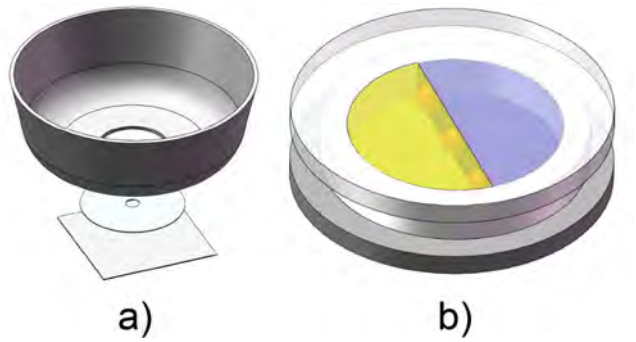

Figure 1. Assembly diagram of microscopic sample cells for the preparation of (a) the horizontal octane/D_2O interface and (b) the vertical octane/D_2O interface.

2.3. Spreading Microspheres at Interfaces via Different Spreading Methods. Two spreading methods were used, including (1) spreading by microinjection that requires spreading solvents and (2) an additive-free spreading method that does not involve spreading solvents. In the microinjection, the suspensions of PS microspheres in D_2O (0.2 μL) containing the spreading solvent (5 vol % isopropanol or 5 vol % methanol) was directly injected into the interface at a flow rate of 0.1 μL/min using a microinjector composed of an *XYZ* manipulator, a syringe pump, and a glass capillary (15−30 μm in diameter). In the additive-free spreading method, the suspension of PS microspheres in D_2O was added before the addition of octane; after

DOI: 10.1021/acs.langmuir.6b01362
Langmuir 2016, 32, 4909−4916

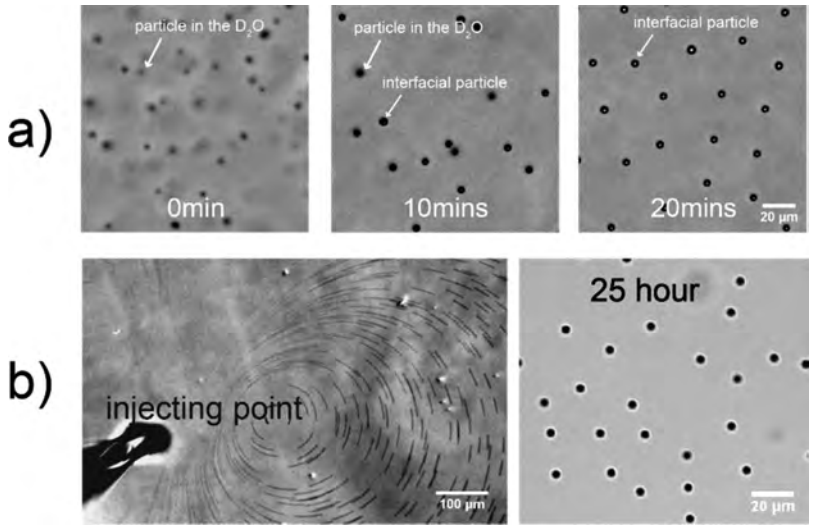

Figure 2. Spreading of PS microspheres to the oil/water interface with different spreading methods. (a) Time series images of spreading PS microspheres to the interface via buoyancy (the additive-free spreading method), where the images (from left to right) were collected at 0, 10, and 20 min, respectively. (b) Representative images of spreading PS microspheres to the interface via the microinjection of particle suspensions (containing 5% isopropanol), where the left image represents the violent spreading of particles at the interface and the right image represents the long-time image (25 h) after spreading.

the addition of octane, the device was placed (20 min) to allow those PS microsperes suspended in D_2O to float to the interface.

2.4. Tracking of Microspheres at Horizontal Oil/Water Interfaces. An inverted microscope (Olympus IX81) equipped with a 10× objective and a sCMOS camera (Andor Zyla) was used to capture bright-field images of those PS microspheres trapped at horizontal oil/D_2O interfaces. The capture rate is 3 s per frame. A data set typically containing 1200 images with a field size of 1664 × 1404 μm^2 was collected. The data sets were continuously collected every 60 min over 15 to 30 h. These experiments were repeated multiple times under identical condition, thus over 120 data sets (>144 000 images) were acquired and analyzed in total, in which the 2560 × 2160 11-bit greyscale images were first converted to binary images for the detection of microsphere with a standard image-processing algorithm coding by MATLAB and the $x-y$ positions of microsphere centroids were subsequently determined and linked individually over time by using a particle-tracking algorithm.[20]

2.5. Measurement of Three-Phase Contact Angle of Microspheres Trapped at Vertical Oil/Water Interfaces. Nonfluorescent polystyrene microspheres (3.5 μm in diameter, surface modification with amidine) were used in both experiments of contact angle measurements and tracking experiments. The microspheres trapped at vertical octane/D_2O interfaces were imaged with an Olympus IX81 inverted microscope equipped with an 100× oil objective. The aqueous phase was labeled with coumarin (10 μM) and then imaged with a high-resolution confocal microscope (Olympus FV1000). Coumarin molecules were excited with a 405 nm laser to acquire confocal images via an emission channel (425−475 nm). The boundaries of the oil/D_2O interface and microspheres were respectively evaluated by finding the maximum intensity gradients from their images. The three-phase contact angle (θ) of a single interfacial particle was geometrically measured using their determinate boundaries, as shown in Figure 3b. To minimize the statistical errors,[21] these experiments were repeated multiple times under identical conditions, thus over 60 confocal images, typically containing 2−4 interfacial particles, were acquired and analyzed in total.

3. RESULTS AND DISCUSSION

3.1. Additive-Free Spreading Method Does Not Drive Particles to Slide along the Interface. Peng et al. have shown that gravity can lead to hydrophobic poly(methyl methacrylate) (PMMA) particle spreading to the decalin/water interface directly by adding particles in the suboil phase, thus enabling one to avoid the use of spreading solvents.[22] Alternatively, we used heavy water (D_2O) to prepare the horizontal oil/water interface, thus expecting that the buoyancy of particles can drive them to float spontaneously to the interface. It is believed that particles can eventually be spread to the interface only if the driving force is able to overcome the resistance forces. Note that the magnitude of the driving force (buoyancy) scales to both the density difference between the particle (1.05 g/cm^3) and D_2O (1.10 g/cm^3) and the volume (the size) of the particle, whereas the resistance force dominated by the repulsions typically consists of the following two facets. First, repulsions could arise from the image charges formed in the oil phase when particles in the subwater phase approach the oil/water interface,[9,23] where the repulsion is independent of the sign of charges located at the particle surface. Second, repulsion could also arise from direct coulomb interactions between the particle and the oil/water interface because the oil/water interface is naturally negatively charged.[24,25] In this case, the repulsion is highly dependent on the sign of charges located at the particle surface. According to the aforementioned facts, we thereby carefully optimized the size and the sign of charges of the used particles. We eventually found that positively charged polystyrene microspheres (surface modification with amidine) with a diameter of 3.5 μm could be spread to the interface quickly (<20 min), as shown in Figure 2a, and that nearly no particles existed in the aqueous phase. By contrast, negatively charged microspheres of the same size could approach only the top of the water phase (adjacent to the interface) rather than spreading to the interface, indicating that direct coulomb interactions between the particle and the oil/water interface play a significant role in preventing particles from spreading to oil/water interfaces. Most importantly, unlike the common process of spreading particles in the presence of spreading solvents (Figure 2b), this additive-free spreading method does not drive particles to slide along the interface. Note that we have optimized these spreading procedures to ensure that the resultant number density of particles arising from these two distinctive methods is as close as possible.

DOI: 10.1021/acs.langmuir.6b01362
Langmuir 2016, 32, 4909−4916

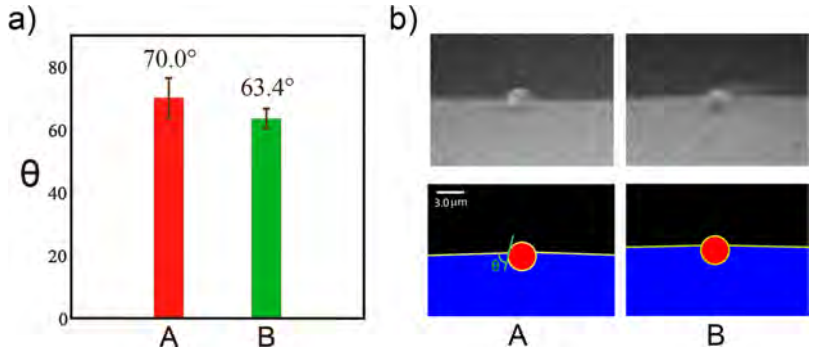

Figure 3. Three-phase contact angle of polystyrene microspheres (3.5 μm) trapped at vertical octane/D_2O interfaces arising from two different spreading methods: (a) statistical results, where symbols A and B represent the results arising from the additive-free spreading method and microinjection, respectively, and (b) representative confocal images, where the gray-scale images are the original images and the blue colors and yellow lines represent the emission of coumarin in the aqueous phase and boundaries determined by finding the maximum gradients of intensities. Three-phase contact angle θ is defined as indicated in A.

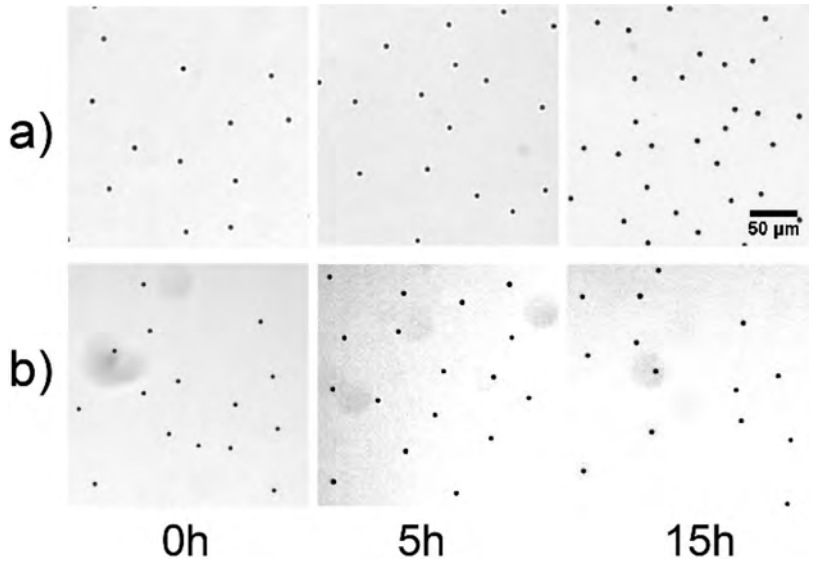

Figure 4. Time evolution of bright-field images of polystyrene microspheres (3.5 μm) trapped at an octane/D_2O interface arising from two different spreading methods. (a) Spreading via the microinjection of particle suspensions at the interface, where the suspensions contain 5% isopropanol. (b) Spreading via the buoyancy that drives particles to float to the interface.

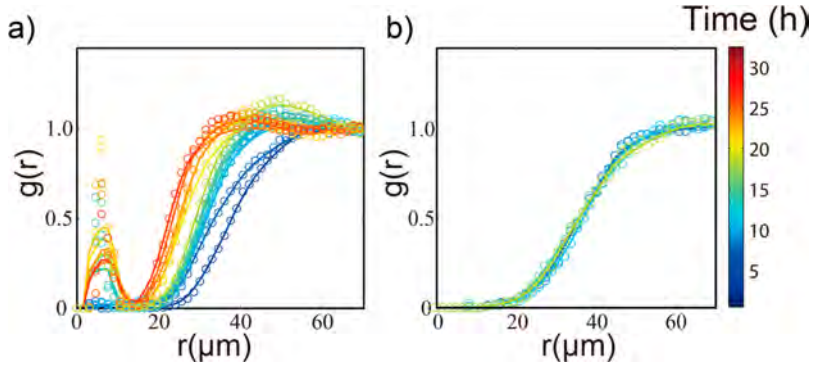

Figure 5. Time evolutions of pair distribution function $g(r)$ of polystyrene microspheres (3.5 μm) trapped at an octane/D_2O interface arising from two different spreading methods. (a) Spreading via the microinjection of particle suspensions at the interface, where the suspensions contain 5% isopropanol. (b) Spreading via the buoyancy that drives particles to float to the interface. Symbols and lines represent original data points and their spline lines, respectively, where the corresponding color indicates the time evolved.

By using confocal microscopy to directly measure the three-phase contact angle (as defined in Figure 3b) of the particles trapped at the oil/D_2O interface,[26,27] we further investigated the influence arising from these two distinctive spreading methods, as shown in Figure 3. It can be seen that using a spreading solvent to spread particles results in a slightly smaller

DOI: 10.1021/acs.langmuir.6b01362
Langmuir 2016, 32, 4909−4916

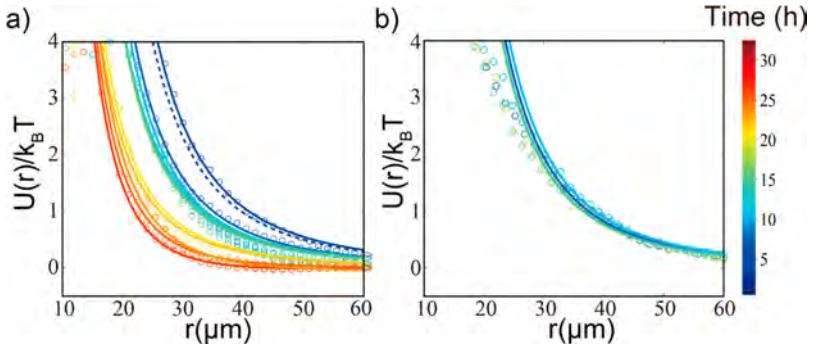

Figure 6. Time evolution of pair potentials $U(r)$ of polystyrene microspheres trapped at an octane/D_2O interface arising from two different spreading methods. (a) Spreading via the microinjection of particle suspensions at the interface, where the suspensions contain 5% isopropanol. (b) Spreading via the buoyancy that drives particles to float to the interface. Symbols and lines represent original data points and fitting curves, respectively, where the corresponding colors indicate the time evolved.

three-phase contact angle ($\theta = 63.4 \pm 2.6°$) comparing to that using the additive-free method ($\theta = 70.0 \pm 6.3°$). Our results indicate that the amphiphilic spreading solvent does affect the wettability of particle at the interface even when its concentration is low, consistent with the literature report.[28] Note that we did not observe a significant deformation of the interface in our experiments, so the capillary force arising from the curvature of the interface can be ignored in this study.[29] Moreover, Figure 3 provides strong evidence to demonstrate that the additive-free method can successfully spread particles to oil/water interfaces.

3.2. Additive-Free Spreading Method Does Not Lead to a Time-Dependent Evolution Feature in Those Interfacial Particles. We noticed that using a spreading solvent to spread particles at oil/water interfaces leads to a time-dependent evolution feature in those interfacial particles; namely, the interfacial particles will approach their neighbors as time evolves (Figure 4a), which is entirely consistent with our previous findings. By contrast, using an additive-free spreading method does not produce the time-dependent evolution feature in those interfacial particles, as shown in Figure 4b. Instead, we found that the shortest approach distance between particle pairs remains constant (~12 μm). To quantify these observations, we measured the pair distribution function $g(r)$ at every sampling time (60 min). Note that the system evolution (if any) is quite slow and the characteristic time is longer than ~5 h. Therefore, $g(r)$ can be calculated from particle positions ($\mathbf{r}_i$) at every sampling time using

$$g(r) = \sum_{i \neq j} \frac{\delta(\mathbf{r}_1 - \mathbf{r}_i)\,\delta(\mathbf{r}_2 - \mathbf{r}_j)}{n} \tag{1}$$

where $r \equiv |\mathbf{r}_1 - \mathbf{r}_2|$ is the separation between particle pairs and n is the number density of particles at the interface. The results of spreading-solvent-involved methods (Figure 5a) clearly indicate that the region of strong negative correlations in the pair distribution function ($g(r) \rightarrow 0$) reaches ~20 μm at the beginning; this negative correlation region gradually decreases as time evolves and reaches a steady value (~12 μm) after 25 h, suggesting that the repulsion among the interfacial particles is gradually attenuated. However, the results of the additive-free spreading method (Figure 5b) show that pair distribution functions remain unchanged over 15 h, indicating that the repulsions among the interfacial particles do not attenuate as time evolves. Note that in neither case did we observe phenomena that implicate an attractive force among those particles.

3.3. Additive-Free Spreading Method Abolishes Residual Charge Formation on the Interfacial Particles. To elucidate why these distinctive spreading methods can lead to different behaviors of those interfacial particles, we directly evaluated pair potentials $U(r)$ among those interfacial particles from $g(r)$ using a hypernetted chain (HCN) approximation,[30] in which $U(r) = -k_BT \ln[g(r)] + nk_BTI(r)$ was applied, where k_B is the Boltzmann constant, T is the absolute temperature, and convolution integral $I(r) = \int [g(r') - 1 - nI(r)][g(|\mathbf{r}' - \mathbf{r}|) - 1]\, d^2r'$ can be obtained iteratively, starting with $I(r) = 0$. Note that in this evaluation we assumed that the system stays in a quasi-equilibrium state at every sampling time. Figure 6 shows that $U(r)$ of the system with an additive-free method remains unchanged over 15 h, which is in sharp contrast to $U(r)$ gradually attenuating with time if one uses a spreading solvent to spread those particles at oil/water interfaces. More importantly, we found that $U(r)$ of system with an additive-free method can be well fit with a minimal theoretical model (the solid lines in Figure 6b) that accounts only for the dipole–dipole interactions among those interfacial particles.[10] In this model, the magnitude of $U(r)$ was determined by only dipole moment Q_{dip} and Debye length λ_D as follows,

$$\frac{U(r)}{k_BT} \approx 8\pi e^{-2} Q_{dip}^{\,2} \left(\frac{l_B^w}{r}\right)\left(\frac{\lambda_D}{r}\right)^2 \tag{2}$$

where e is the elementary charge, $l_B^w = e^2/4\pi\varepsilon_w\varepsilon_w k_BT$ is the Bjerrum length in water, and ε_w and ε_0 are the permittivities of water and vacuum, respectively. However, eq 2 cannot be used to fit $U(r)$ in the relative short range ($r < 40$ μm) if one uses a spreading solvent to spread those particles at oil/water interfaces, as shown in Figure 6a (the dashed line). Instead, we found that a combination of eq 2 and a second term $\frac{U(r)}{k_BT} \approx 4\pi e^{-2} Q_{res}^{\,2}\left(\frac{l_B^o}{r} - \frac{l_B^o}{\sqrt{4a^2 + r^2}}\right)$ that further accounts for the residual charges Q_{res} located in the oil phase at a distance a can well fit $U(r)$ over the full range (solid lines in Figure 6a),[13] indicating that $U(r)$ was actually dominated by the second term in the relative short range, where l_B^o is the Bjerrum length in oil. The consistency with the fittings and experimental data strongly suggests that the additive-free spreading method does not lead to residual charges forming on those interfacial particles at oil/water interfaces. To further demonstrate that, we added 10 mM sodium chloride to the subphase of heavy

DOI: 10.1021/acs.langmuir.6b01362
Langmuir 2016, 32, 4909–4916

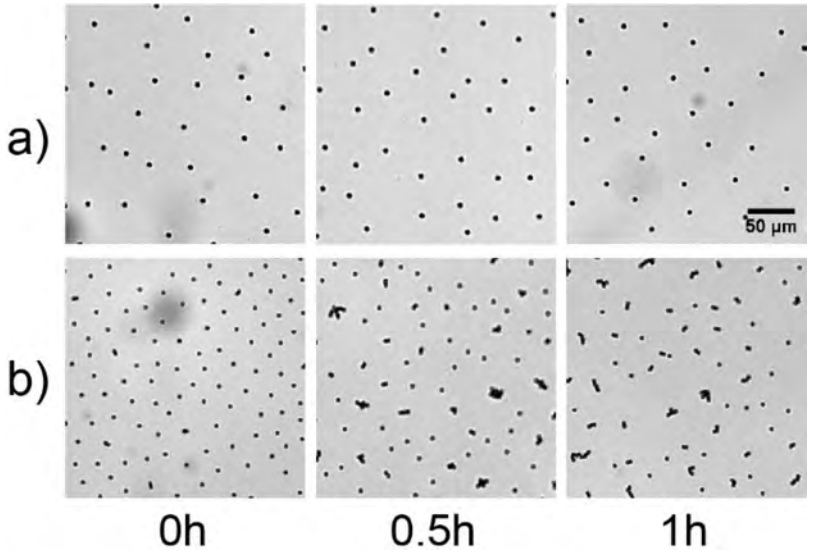

Figure 7. Time evolution of bright-field images of polystyrene microspheres (3.5 μm) trapped at an octane/D_2O interface arising from two different methods, where the aqueous phase contains 10 mM NaCl: (a) via microinjection and (b) via the additive-free spreading method.

water to screen the repulsions arising from the dipole−dipole interactions. We found that the particles would aggregate quickly (<30 min) at the interface if the additive-free spreading method was employed (Figure 7b) but particles would remain stable in the first hour if spreading solvent was employed (Figure 7a). This result thus provides additional evidence that the additive-free spreading method does not lead those unscreened charges to form in the oil subphase.

3.4. Additional Effects Arising from the Spreading Solvents. We noticed that even after sufficient time (>25 h), repulsion among the particles arising from the additive-free method is relative stronger than that arising from the method involved using spreading solvents, as shown in Figure 6, which suggests that adding the spreading solvent causes additional effects on those interfacial particles. It has been known that adding the spreading solvents can change the three-phase contact angle of particles trapped at oil/water interfaces, thus further affecting their interactions at the interface. Actually, we found that using a spreading solvent to spread the particles onto the interface would result in a slightly smaller three-phase contact angle (θ = 63.4 ± 2.6°) than that (θ = 70.0 ± 6.3°) arising from the additive-free spreading method. One can expect that exposing a larger portion of an interfacial particle to the aqueous phase (θ < 90°) could attenuate its dipole moment, thus repressing dipole−dipole repulsions among the interfacial particles. As expected, our results indicate that (Figures 6 and 8b) the dipole−dipole repulsion arising from adding spreading solvent is weaker than that arising from the additive-free method. Aside from affecting the wettability of particles at the interface, it is also argued that the spreading solvent (isopropanol) may swell the polystyrene particles and change the surface structure of the particles. To further address this point, we used methanol instead of isopropanol as the spreading solvent in the spreading procedure because methanol is milder for polystyrene than is isopropanol. Therefore, one can expect that methanol would lead to a smaller swelling effect if it exists. We found that using methanol as the spreading solvent can reproduce similar results arising from using isopropanol, including the time-dependent feature of $U(r)$ (Figure 8a) and a similar three-phase contact angle (data not shown). Interestingly, we found that the resultant dipole−dipole repulsion arising from using methanol is stronger than that arising from using isopropanol after waiting a sufficient time (~25 h) but is still weaker than that arising from using the additive-free method, as shown in Figure 8b. These findings suggested that (1) the swelling effect arising from isopropanol cannot be ignored at an oil/water interface and (2) using a spreading solvent does affect the wettability of particles at the interface, thus further affecting the interactions among those particles.

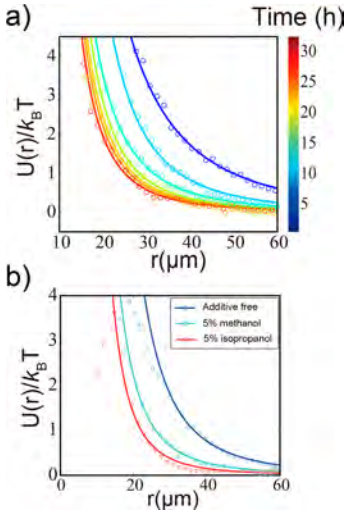

Figure 8. (a) Time evolution of pair potential $U(r)$ of polystyrene microspheres (3.5 μm) trapped at an octane/D_2O interface spreading via the microinjection of particle suspensions at the interface, where the suspension contains 5% methanol. (b) Pair potential $U(r)$ of polystyrene microspheres trapped at an octane/D_2O interface 25 h after spreading, where the suspension contains 5% isopropanol or 5% methanol or spreading via the buoyancy that drive particles to float to the interface. Symbols and lines represent original data points and fitting curves, respectively, where their colors indicate the time evolved.

DOI: 10.1021/acs.langmuir.6b01362
Langmuir 2016, 32, 4909−4916

4. CONCLUSIONS

In this study, we investigated the influence of spreading solvent on the interactions between charged colloidal particles at an oil/water interface. Our results showed that the essential difference between the additive-free spreading method and the methods requiring spreading solvents is that the additive-free spreading method does not lead particles to slide along the interface, which is in sharp contrast to particles sliding violently at the interface if a spreading solvent is applied to spread the particles. We have shown that this difference results in distinctive interfacial behavior; namely, violently sliding of particles at the interface leads to the emergence of unstable residual charges in the oil phase, whereas particles that float to the interface (avoiding sliding) do not cause the formation of residual charges. These findings agree well with our previous hypothesis that the unstable residual charges actually arise from the violent rubbing of particles against oil at the interface. Most importantly, the additive-free spreading method has been demonstrated to be able to completely abolish the formation of those unstable residual charges in the oil phase, which is crucial to applying the system of microsized particles trapped at oil/water interfaces to ongoing investigations that require precise control of the interfacial interactions among colloidal particles.

AUTHOR INFORMATION

Corresponding Authors

*E-mail: tongai@cuhk.edu.hk.
*E-mail: fjinustc@ustc.edu.cn.

Author Contributions

P.G. and Z.Y. contributed equally.

Notes

The authors declare no competing financial interest.

ACKNOWLEDGMENTS

This work was supported by the National Natural Science Foundation of China (21104071), the Fundamental Research Funds for the Central Universities (WK2030020023, WK2340000066), the Specialized Research Fund for the Doctoral Program of Higher Education (20133402110034), the National Natural Science Foundation of China (21374091), and the Shenzhen Science and Technology Innovation Committee for the Municipal Key Laboratory Scheme (ZDSY20130401150914965).

REFERENCES

(1) Zhang, Z.; Xu, N.; Chen, D. T. N.; Yunker, P.; Alsayed, A. M.; Aptowicz, K. B.; Habdas, P.; Liu, A. J.; Nagel, S. R.; Yodh, A. G. Thermal vestige of the zero-temperature jamming transition. *Nature* **2009**, *459* (7244), 230−233.

(2) Zahn, K.; Lenke, R.; Maret, G. Two-stage melting of paramagnetic colloidal crystals in two dimensions. *Phys. Rev. Lett.* **1999**, *82* (13), 2721−2724.

(3) Basavaraj, M. G.; Fuller, G. G.; Fransaer, J.; Vermant, J. Packing, flipping, and buckling transitions in compressed monolayers of ellipsoidal latex particles. *Langmuir* **2006**, *22* (15), 6605−6612.

(4) Loudet, J. C.; Alsayed, A. M.; Zhang, J.; Yodh, A. G. Capillary interactions between anisotropic colloidal particles. *Phys. Rev. Lett.* **2005**, *94* (1), 018301.

(5) Dickinson, E. Food emulsions and foams: Stabilization by particles. *Curr. Opin. Colloid Interface Sci.* **2010**, *15* (1−2), 40−49.

(6) Dinsmore, A. D.; Hsu, M. F.; Nikolaides, M. G.; Marquez, M.; Bausch, A. R.; Weitz, D. A. Colloidosomes: Selectively permeable capsules composed of colloidal particles. *Science* **2002**, *298* (5595), 1006−1009.

(7) Verma, A.; Uzun, O.; Hu, Y.; Hu, Y.; Han, H.-S.; Watson, N.; Chen, S.; Irvine, D. J.; Stellacci, F. Surface-structure-regulated cell-membrane penetration by monolayer-protected nanoparticles. *Nat. Mater.* **2008**, *7* (7), 588−595.

(8) Verma, A.; Stellacci, F. Effect of surface properties on nanoparticle-cell interactions. *Small* **2010**, *6* (1), 12−21.

(9) Leunissen, M. E.; van Blaaderen, A.; Hollingsworth, A. D.; Sullivan, M. T.; Chaikin, P. M. Electrostatics at the oil-water interface, stability, and order in emulsions and colloids. *Proc. Natl. Acad. Sci. U. S. A.* **2007**, *104* (8), 2585−2590.

(10) Pieranski, P. Two-dimensional interfacial colloidal crystals. *Phys. Rev. Lett.* **1980**, *45* (7), 569−572.

(11) Petkov, P. V.; Danov, K. D.; Kralchevsky, P. A. Monolayers of charged particles in a Langmuir trough: Could particle aggregation increase the surface pressure? *J. Colloid Interface Sci.* **2016**, *462*, 223−234.

(12) Petkov, P. V.; Danov, K. D.; Kralchevsky, P. A. Surface Pressure Isotherm for a Monolayer of Charged Colloidal Particles at a Water/Nonpolar-Fluid Interface: Experiment and Theoretical Model. *Langmuir* **2014**, *30* (10), 2768−2778.

(13) Aveyard, R.; Clint, J. H.; Nees, D.; Paunov, V. N. Compression and structure of monolayers of charged latex particles at air/water and octane/water interfaces. *Langmuir* **2000**, *16* (4), 1969−1979.

(14) Aveyard, R.; Binks, B. P.; Clint, J. H.; Fletcher, P. D. I.; Horozov, T. S.; Neumann, B.; Paunov, V. N.; Annesley, J.; Botchway, S. W.; Nees, D.; Parker, A. W.; Ward, A. D.; Burgess, A. N. Measurement of long-range repulsive forces between charged particles at an oil-water interface. *Phys. Rev. Lett.* **2002**, *88* (24), 246102.

(15) Masschaele, K.; Park, B. J.; Furst, E. M.; Fransaer, J.; Vermant, J. Finite Ion-Size Effects Dominate the Interaction between Charged Colloidal Particles at an Oil-Water Interface. *Phys. Rev. Lett.* **2010**, *105* (4), 048303.

(16) Uppapalli, S.; Zhao, H. The influence of particle size and residual charge on electrostatic interactions between charged colloidal particles at an oil-water interface. *Soft Matter* **2014**, *10* (25), 4555−4560.

(17) Law, A. D.; Auriol, M.; Smith, D.; Horozov, T. S.; Buzza, D. M. A. Self-Assembly of Two-Dimensional Colloidal Clusters by Tuning the Hydrophobicity, Composition, and Packing Geometry. *Phys. Rev. Lett.* **2013**, *110* (13), 138301.

(18) Gao, P.; Xing, X. C.; Li, Y.; Ngai, T.; Jin, F. Charging and discharging of single colloidal particles at oil/water interfaces. *Sci. Rep.* **2014**, *4*, 4778.

(19) Birikh, R. V.; Denisova, M. O.; Kostarev, K. G. The Development of Marangoni Convection Induced by Local Addition of a Surfactant. *Fluid Dyn.* **2011**, *46* (6), 890−900.

(20) Jin, F.; Conrad, J. C.; Gibiansky, M. L.; Wong, G. C. L. Bacteria use type-IV pili to slingshot on surfaces. *Proc. Natl. Acad. Sci. U. S. A.* **2011**, *108* (31), 12617−12622.

(21) Snoeyink, C.; Barman, S.; Christopher, G. F. Contact Angle Distribution of Particles at Fluid Interfaces. *Langmuir* **2015**, *31* (3), 891−897.

(22) Peng, Y.; Chen, W.; Fischer, T. M.; Weitz, D. A.; Tong, P. Short-time self-diffusion of nearly hard spheres at an oil-water interface. *J. Fluid Mech.* **2009**, *618*, 243−261.

(23) Wang, H.; Singh, V.; Behrens, S. H. Image Charge Effects on the Formation of Pickering Emulsions. *J. Phys. Chem. Lett.* **2012**, *3* (20), 2986−2990.

(24) Roger, K.; Cabane, B. Why Are Hydrophobic/Water Interfaces Negatively Charged? *Angew. Chem., Int. Ed.* **2012**, *51* (23), 5625−5628.

(25) Marinova, K. G.; Alargova, R. G.; Denkov, N. D.; Velev, O. D.; Petsev, D. N.; Ivanov, I. B.; Borwankar, R. P. Charging of oil-water interfaces due to spontaneous adsorption of hydroxyl ions. *Langmuir* **1996**, *12* (8), 2045−2051.

(26) Sundberg, M.; Mansson, A.; Tagerud, S. Contact angle measurements by confocal microscopy for non-destructive microscale

DOI: 10.1021/acs.langmuir.6b01362
Langmuir 2016, 32, 4909−4916

surface characterization. *J. Colloid Interface Sci.* **2007**, *313* (2), 454−460.
(27) Mohammadi, R.; Amirfazli, A. Contact angle measurement for dispersed microspheres using scanning confocal microscopy. *J. Dispersion Sci. Technol.* **2005**, *25* (5), 567−574.
(28) Maestro, A.; Bonales, L. J.; Ritacco, H.; Rubio, R. G.; Ortega, F. Effect of the spreading solvent on the three-phase contact angle of microparticles attached at fluid interfaces. *Phys. Chem. Chem. Phys.* **2010**, *12* (42), 14115−14120.
(29) Yao, L.; Sharifi-Mood, N.; Liu, I. B.; Stebe, K. J. Capillary migration of microdisks on curved interfaces. *J. Colloid Interface Sci.* **2015**, *449*, 436−442.
(30) Behrens, S. H.; Grier, D. G. Pair interaction of charged colloidal spheres near a charged wall. *Phys. Rev. E: Stat. Phys., Plasmas, Fluids, Relat. Interdiscip. Top.* **2001**, *64* (5), 050401.

DOI: 10.1021/acs.langmuir.6b01362
Langmuir 2016, 32, 4909−4916